

## Supporting Information

# Conformally Coated Nickel Phosphide on 3D, Ordered Nanoporous Nickel for Highly Active and Durable Hydrogen Evolution

*Anand P. Tiwari,<sup>‡1</sup> Kisung Lee,<sup>‡1</sup> Kisun Kim,<sup>1</sup> Jin Kim,<sup>1</sup> Travis G. Novak,<sup>1</sup> and Seokwoo Jeon<sup>\*1</sup>*

1. Department of Materials Science and Engineering, KAIST Institute for the Nanocentury, Advanced Battery Center, KAIST, Daejeon 305-701, Republic of Korea.

### **Corresponding Author**

\*Prof. Seokwoo Jeon: [jeon39@kaist.ac.kr](mailto:jeon39@kaist.ac.kr)

In this supplement, we provide the data and description, which support to our main text.

Number of pages: 7

Number of Figures: 8

Number of Tables: 2

## Experimental Procedures

*Material Synthesis:* Firstly, 3D continuous periodic nanostructure polymer template is prepared by well-known PnP technique.<sup>1-4</sup> Briefly, a photoresist polymer 3D nanopatterns is fabricated and coated with Ni by electrodeposition. Finally, the photoresist polymer is etched by developing solution. Synthesis of Ni<sub>2</sub>P on Ni is done by annealing with red phosphorous (P) in tube furnace at 500 °C for 45 min. Firstly, the 3D Ni is cleaned with acetic acid to remove surface oxide layers then placed in the tube furnace with 0.025 g of red P placed 2 cm away 3D Ni at the upstream side. Tube furnace is purged with Ar at a flow rate of 100 SCCM for 30 min. Then the furnace is heated to 500 °C at 5 °C·min<sup>-1</sup>, and kept at this temperature for 45 min and cooled down to 250 °C at same rate and maintained at this temperature for 3 h. Finally, the furnace is naturally cooled down to room temperature. Ar was kept flowing in tube furnace through all processes.

*Chemical and Microstructural Characterizations:* The nanostructures, morphology, crystal structures and, chemical states of as-prepared nano-patterns are investigated by a transmission electron microscope (TEM), a field-emission scanning electron microscope (FESEM) (FBI company, Magellen400), a thin film X-ray diffractometer (XRD) (Cu  $\alpha$ 1 radiation, (Rigaku, SmarLab)), and X-ray photospectroscopy (Thermo VG Scientific, K-alpha).

*Electrochemical Characterizations:* Electrocatalytic experiment are done by VersaSTATE 3 (principle applied research) electrochemical workstation with a well-known three-electrode systems (working electrode was as-prepared nano-patterns, the reference electrode was Ag/AgCl in 3M KCl, and the counter electrode was a Pt wire) in 0.5 M H<sub>2</sub>SO<sub>4</sub> electrolyte for HER activity.<sup>5</sup> It is worth to noting that nano-patterns were directly connected as working electrode without adding any binder. All of the potentials were calibrated to a RHE,  $E_{(RHE)} = E_{Ag/AgCl} + 0.059 \text{ pH} + E^0_{Ag/AgCl}$ , where  $E^0_{Ag/AgCl} = 0.1976 \text{ V}$ .

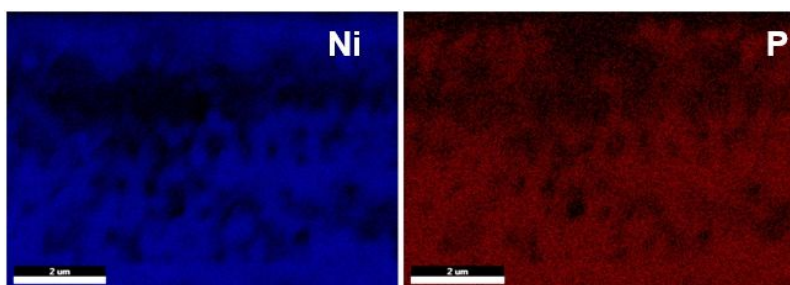


**Figure S1.** EDX elemental mapping of as-prepared 3DN-Ni<sub>2</sub>P-Ni nano-patterns.

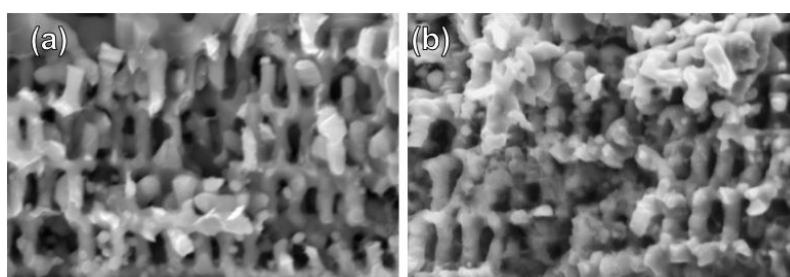


**Figure S2.** Cross-sectional SEM images (a) 3DN-Ni<sub>2</sub>P, and (b) 3DN-M-NiP nano-patterns.

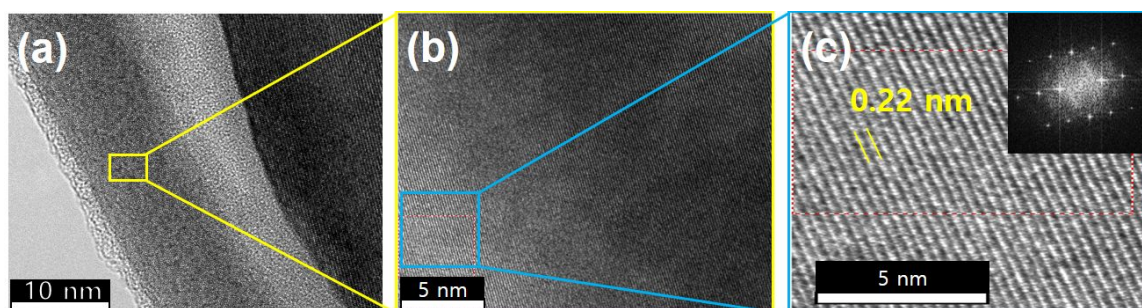


**Figure S3.** (a) TEM images of 3DN-Ni<sub>2</sub>P-Ni nano-patterns. (b) Magnified image of Ni<sub>2</sub>P region. (c) Fast Fourier transforms (FFT) for Ni<sub>2</sub>P magnified region, showing the line profile of Ni<sub>2</sub>P.

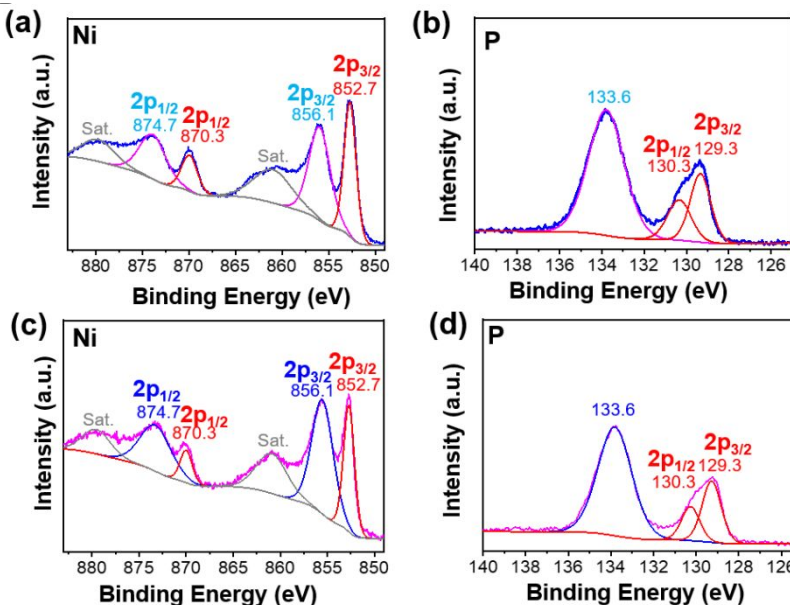


**Figure S4:** (a) Ni 2p, and (b) P 2p XPS spectra for 3DN-Ni<sub>2</sub>P. Blue line in the XPS is raw data, and other colored lines are fit components. (c) Ni 2p, and (d) P 2p XPS spectra for 3DN-M-NiP. Magenta line in the XPS is raw data, and other colored lines are fit components.

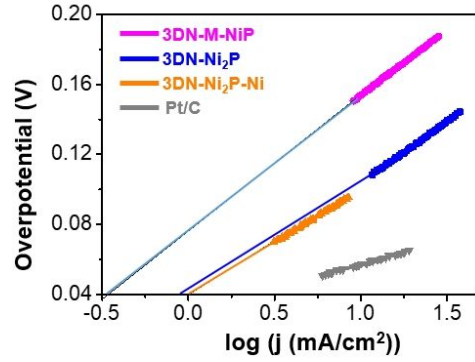


**Figure S5.** Tafel plots of as-prepared 3D nano-patterns to calculate exchange current density.

Exchange current density ( $j_0$ ) is calculated by following Butler-Volmer equation:

$$j = j_0 [e^{-\alpha n f \eta} - e^{(1-\alpha) n f \eta}] \quad (1)$$

Where  $j_0$  is the exchange current density,  $\eta$  is overpotentials,  $\alpha$  is transfer coefficient,  $n$  is the electron transfer number,  $f$  is denoted as  $F/RT$  ( $F$ : Faraday constant;  $R$ : the gas constant;  $T$ : the absolute temperature). Our study is focused on cathodic HER, the anodic OER contributing current is considered as negligible, so the second part of equation (1) will be zero. And then the equation will be:

$$\eta = \frac{2.3RT}{\alpha n f} \log J - \frac{2.3RT}{\alpha n f} \log j_0 \quad (2)$$

$$\alpha = \frac{2.3RT}{\alpha n f} \log j_0 \quad (3)$$

According to the above equation  $j_0$  can be calculated from the intercept of the Tafel plot, shown in Figure S3.

**Description to calculate turn over frequency (TOF) for  $H_2$  of as-prepared nano-patterns:**

The structural data of  $Ni_2P$  from the ICDD-PDF-4 + (JCPDS 65-3544) database is used.

Density of  $Ni_2P = 7.200 \text{ g cm}^{-3}$ . Average size of  $Ni_2P$  nanoparticle (determined from the Scherrer equation) = 20 nm. The shapes of the nanoparticles are approximated to spherical.

The volume of the 1 nano-pore in the 3D nano patterns is  $3.14 \times 10^{-12} \text{ cm}^3$ . The number of nano-pores in the electrode is  $10^{12}$ . In addition, the loading amount of material on electrode is  $1 \text{ mg/cm}^2$ . Total volume of  $Ni_2P$  particles present on the electrode

$$= ((1 \times 10^{-5}) / 7.20) \times 3.14 = 4.3 \times 10^{-6} \text{ cm}^3$$

Total number of  $Ni_2P$  nanoparticles present on the electrode

$$= (4.3 \times 10^{-6}) / [(4/3) (\pi) (r^3)]$$

$$= (4.3 \times 10^{-6}) / [4.18 \times (10 \times 10^{-7})^3]$$

$$= 1.02 \times 10^{12} \text{ particles}$$

Surface area of one  $Ni_2P$  nanoparticle

$$= (4) (\pi) (r^2)$$

$$= 1.25 \times 10^{-15} \text{ m}^2$$

Total surface area of all  $Ni_2P$  the nanoparticles present

$$= (1.02 \times 10^{12}) \times (1.25 \times 10^{-15}) = 1.28 \times 10^{-3} \text{ m}^2$$

The area of per unit cells of  $Ni_2P = 1.914 \times 10^{-19} \text{ m}^2$

There are 3.5 Ni atoms in this cell.

Total number of Ni atoms presents

$$= [3.5 / (1.914 \times 10^{-19})] \times (1.28 \times 10^{-3})$$

$$= 2.32 \times 10^{16} \text{ atoms}$$

After dividing effective atoms by total number of particles, we can get turn over frequency at particular potentials.

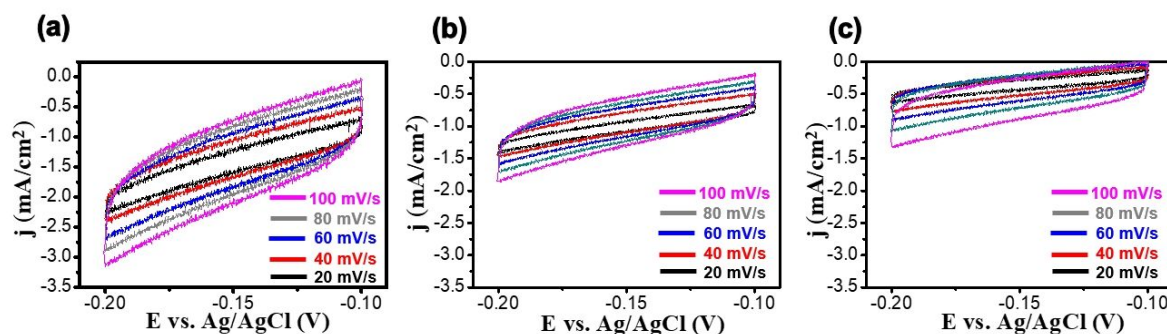


**Figure S6.** Cyclic voltammetry at different scan rate for (a) 3DN-Ni<sub>2</sub>P-Ni, (b) 3DN-Ni<sub>2</sub>P, and (c) 3DN-M-NiP nano-patterns in 0.5 M H<sub>2</sub>SO<sub>4</sub> electrolyte.

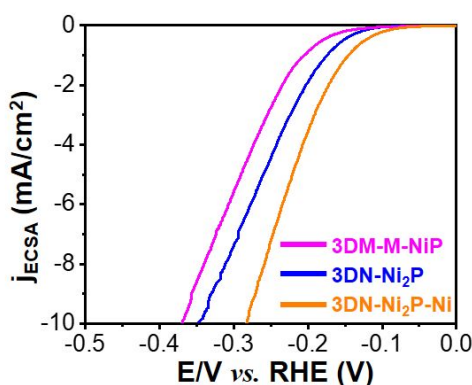


**Figure S7.** Polarization curves of as-prepared 3D nano-patterns normalized by ECSA.

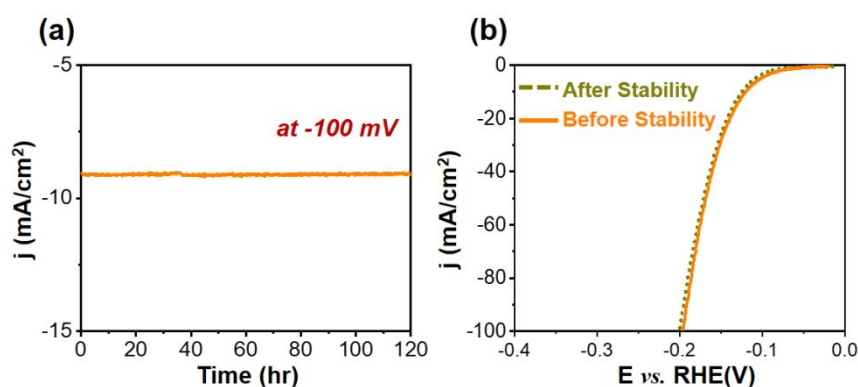


**Figure S8.** Electrochemical stability test using graphite rod as counter electrode. (a) Chronoamperometry for 3DN-Ni<sub>2</sub>P-Ni. (b) Polarization curve of 3DN-Ni<sub>2</sub>P-Ni before and after stability test.

**Supporting Table S1.** Comparison of electrocatalytic activity for HER of 3DN-Ni<sub>2</sub>P-Ni with recently reported nickel phosphide based catalysts in 0.5 M H<sub>2</sub>SO<sub>4</sub>.

Catalysts	Over potential at 10 mA/cm <sup>2</sup> ( $\eta_{10}$ (mV))	Tafel slope (mV dec <sup>-1</sup> )	References

Ni <sub>5</sub> P <sub>4</sub> -Ni <sub>2</sub> P foam	131	79	<i>Nano Energy</i> <b>2019</b> , 55, 193-202.
Ni-Ni <sub>x</sub> P on Carbon Cloth	164	76	<i>Electrochim. Acta</i> <b>2019</b> , 298, 229–236.
Ni <sub>x</sub> P/CNT	150	61	<i>Nano Res.</i> <b>2017</b> , 10, 415–425.
Single-phase Ni <sub>5</sub> P <sub>4</sub> on Cu-foam	90	49	<i>J. Mater. Chem. A</i> <b>2019</b> , 7, 23989-23999.
Ni <sub>5</sub> P <sub>4</sub> -Ni <sub>2</sub> P-NS	120	79	<i>Angew. Chem. Int. Ed.</i> <b>2015</b> , 54, 8188-8192.
Ni <sub>2</sub> P/CNT	125	64	<i>Adv. Funct. Mater.</i> <b>2016</b> , 26, 7170-7177.
p-doped carbon at Ni <sub>2</sub> P in graphene	110	58	<i>J. Mater. Chem. A</i> , <b>2018</b> , 6, 24107-24113
Ni <sub>2</sub> P/CNT	124	53	<i>J. Mater. Chem. A</i> <b>2015</b> , 3, 13087-13094
Ni <sub>5</sub> P <sub>4</sub> nano sheets on Ni	140	53	<i>Angew. Chem. Int. Ed.</i> <b>2015</b> , 54, 12361 –12365.
Ni-P on Carbon Fiber	98	58	<i>Adv. Funct. Mater.</i> <b>2016</b> , 26, 4067–4077.
Ni <sub>2</sub> P/Ni-Foam	225	112	<i>ACS Sustainable Chem. Eng.</i> <b>2019</b> , 7, 12770–12778.
<b>3DN-Ni<sub>2</sub>P-Ni</b>	<b>101</b>	<b>60</b>	<b>This Work</b>

**Supporting Table S2.** Comparison of the TOF value of 3DN-Ni<sub>2</sub>P-Ni with other reported catalysts.

Catalysts	Electrolyte	TOF at $\eta=100$ m V (s <sup>-1</sup> )	References
CoP	0.5 H <sub>2</sub> SO <sub>4</sub>	0.046	<i>Angew. Chem. Int. Ed.</i> <b>2014</b> , 53, 5427-5430.
Co-NG	0.5 H <sub>2</sub> SO <sub>4</sub>	0.101	<i>Nat. Commun.</i> <b>2016</b> , 6, 8668.
CoN <sub>x</sub> /C	0.5 H <sub>2</sub> SO <sub>4</sub>	0.39	<i>Nat. Commun.</i> <b>2015</b> , 6, 7992.
NiCo <sub>2</sub> P <sub>x</sub>	1 M KOH	0.056	<i>Adv. Mater.</i> <b>2017</b> , 29, 1605502.
Pt/C	0.5 H <sub>2</sub> SO <sub>4</sub>	1.25	<i>Energy Environ. Sci.</i> <b>2018</b> , 11, 1232-1239.
PtRu/RFCS	0.5 H <sub>2</sub> SO <sub>4</sub>	0.375	<i>Energy Environ. Sci.</i> <b>2018</b> , 11, 1232-1239.
CoP/CC	1 M PBS	0.725 (75 mV)	<i>Angew. Chem. Int. Ed.</i> <b>2014</b> , 53, 5427-5430.
CoP <sub>x</sub>	1 M KOH	0.015	<i>Adv. Mater.</i> <b>2017</b> , 29, 1605502.

p-1T-MoS <sub>2</sub>	0.5 H <sub>2</sub> SO <sub>4</sub>	0.5 (153 mV)	<i>J. Am. Chem. Soc.</i> <b>2016</b> , <i>138</i> , 7965-7972.
Ni <sub>2</sub> P	1 M KOH	0.006	<i>Nano Energy</i> <b>2018</b> , <i>53</i> , 492–500.
Ni <sub>2(1-x)</sub> P	1 M KOH	0.038	<i>Nano Energy</i> <b>2018</b> , <i>53</i> , 492–500.
Ni <sub>2</sub> P/CNT	0.5 H <sub>2</sub> SO <sub>4</sub>	0.1 (170 mV)	<i>J. Mater. Chem. A</i> <b>2015</b> , <i>3</i> , 13087-13094
Ni <sub>12</sub> P <sub>5</sub> /CNT	0.5 H <sub>2</sub> SO <sub>4</sub>	0.1 (254 mV)	<i>J. Mater. Chem. A</i> <b>2015</b> , <i>3</i> , 13087-13094
<b>3DN-Ni<sub>2</sub>P-Ni</b>	<b>0.5 H<sub>2</sub>SO<sub>4</sub></b>	<b>0.87</b>	<b>This Work</b>

### Supporting Information References:

1. Ahn, C.; Kim, S. M.; Jung, J. W.; Park, J.; Kim, T.; Lee, S. E.; Jang, D.; Hong, J. W.; Han, S. M.; Jeon, S. Multifunctional Polymer Nanocomposites Reinforced by 3D Continuous Ceramic Nanofillers. *ACS Nano* **2018**, *12*, 9126-9133.
2. Hyun, G.; Cho, S. H.; Park, J.; Kim, K.; Ahn, C.; Tiwari, A. P.; Kim, I. -D.; Jeon, S. 3D ordered carbon/SnO<sub>2</sub> hybrid nanostructures for energy storage applications. *Electrochim. Acta* **2018**, *288*, 108-114.
3. Lee, K.; Yoon, H.; Ahn, C.; Park, J.; Jeon, S. Strategies to improve the photocatalytic activity of TiO<sub>2</sub>: 3D nanostructuring and heterostructuring with graphitic carbon nanomaterials. *Nanoscale*, **2019**, *11*, 7025-7040.
4. Kim, K.; Tiwari, A. P.; Hyun, G.; Novak, T. G.; Jeon, S. Improving electrochemical active area of MoS<sub>2</sub> via attached on 3D-ordered structures for hydrogen evolution reaction. *Int. J. Hydrogen Energy* **2019**, *44*, 28143-28150.
5. Kim, S.; Ahn, C.; Cho, Y.; Hyun, G.; Jeon, S.; Park, J. H. Suppressing buoyant force: New avenue for long-term durability of oxygen evolution catalysts. *Nano Energy* **2018**, *54*, 184-191.